JOURNAL OF MATERIALS SCIENCE 29 (1994) 3612–3620

Information given by slow melting on phase content and maximum drawability of high molecular weight polyethylene films

H. PHUONG-NGUYEN, G. DELMAS
Université du Québec à Montréal, Département de chimie, CP 8888, Succ. A., Montréal, Québec, Canada H3C 3P8

The technique of slow melting ($v = 1\ K\ h^{-1}$) used previously on nascent high molecular weight PE (UHMWPE) is now applied to films prepared in different solvents. Besides the expected endotherm of fusion of the orthorhombic crystals, new endotherms and phase changes are observed at low and high temperature. The total enthalpy of phase change is near the enthalpy of melting of perfect orthorhombic crystals. The new endotherms with slower kinetics can be distinguished on the melting trace from the melting of the orthorhombic crystals. The trace permits the definition of a calorimetric phase composition of a sample. The different films have the same amount of orthorhombic crystals but different phase compositions. Their maximum drawability λ_{max} is solvent-dependent and varies between 260 (n-C_{12}) and 60 (trichlorobenzene). The comparison of calorimetric spectra and values λ_{max} suggests the existence of an optimum in the range of phase-change temperatures to obtain a high λ_{max}. The melting traces of drawn films show that the temperature of the high-T endotherms is lowered by drawing. The phase content of nascent UHMWPE is dramatically changed by melting–recrystallization. The origin of the non-orthorhombic phase changes is discussed.

1. Introduction

In order to understand better the mechanism of dissolution of crystals and gel formation on cooling for high molecular weight polyethylene (UHMWPE), heats of dissolution of nascent UHMWPE have been obtained [1] using a sensitive and stable calorimeter able to accommodate large cells. Dissolution was achieved at low rates of heating (1–3 $K\ h^{-1}$) because otherwise the solution of this high MW was not homogeneous. The same slow-T ramp was used also for melting UHMWPE [2]. In either case, high-T endotherms with a slow kinetics of evolution have been found.

Analysis of other PE samples of medium and low MW [2–4] and of other polyolefins [4, 5] showed that the effect exists on samples melted and recrystallized and on a variety of polymers. The present work, which gives melting traces of dried films prepared in different solvents, is a continuation of previous work on nascent polymer but the emphasis has been shifted to the role of solvent used for the preparation of the films on their morphology and maximum drawability λ_{max}. The possibility that the solvents could change the morphology of the polymer and influence its drawability could be deduced from literature data [6–14] and our work on dissolution and solution properties in different solvents [8] of nascent sample. The solvent profoundly changes the sample morphology since drawability is dramatically increased by the gel route. Although a variety of techniques has been used to understand the morphology of drawable films, the conditions to achieve high-quality fibres [9–21] and the process of drawing [17], some ambiguity remains concerning the changes brought in the polymer by dissolution–recrystallization. This paper presents the case of a technique of slow calorimetry which can follow phase changes in the non-orthorhombic part of the sample and also establish its phase composition.

2. Experimental procedure

2.1. Materials

The polymers investigated were as in previous work [1, 2, 8], namely PE Hostalen Gur 413 (Hoechst) with a nominal value of M_W equal to 900 000 and lower M_W samples such as Marlex ($M_W = 150\,000$, $M_W/M_n \simeq 10$) and NIST 1484 ($M_W = 119\,000$, $M_W/M_n = 1.19$).

The solvents were decalin, dodecane (n-C_{12}), hexadecane (n-C_{16}), 2,2,4,4,6,8,8-heptamethylnonane (br-C_{16}), trichlorobenzene (TCB) and chloronaphthalene, all used without purification. Their purity was indicated by Aldrich to be 99%.

2.2. Apparatus

Slow calorimetry was performed in the sensitive and stable C80 Setaram calorimeter. The sample (8–15 mg) was placed on Hg in a glass tube, subsequently sealed after bubbling N_2 during 2 h. The

0022–2461

temperature ramp was initiated after a 17 h equilibrium time in the calorimeter at 100 °C for $v = 1\ K\ h^{-1}$ and at 50 °C for $v = 6\ K\ h^{-1}$.

Fast calorimetry was achieved in a Perkin-Elmer DSC-2C calibrated with indium. Some drawn samples were constrained before fusion by sandwiching them into two aluminium foils subsequently folded several times. For the sake of brevity, the changes of enthalpy are written as H and not ΔH.

Density values were measured at 25 °C in a mixture of benzene and trichlorobenzene. The density of the mixture in equilibrium with the sample was obtained with an Anton Paar vibrating cell densimeter.

Small angle X-ray scattering was recorded with a Rigaku-Denki pinhole collimator vacuum camera using a CuK_α radiation with a nickel filter. Birefringence measurements were carried out on a Reichert polarization microscope equipped with a Babinet compensator.

Drawing was performed on an Instron tensile tester equipped with a hot-air oven. The strips (30 mm × 8–10 mm) were stretched at 120 °C with a crosshead speed of 20 mm min^{-1}. The Young's modulus E was obtained at room temperature, the initial sample length being 30 mm and the stretching speed 20 mm min^{-1}.

The Young's modulus, E, and the birefringence, B, depend mainly on the value of λ and not on the solvent in which they are prepared. The dependencies $E(\lambda)$ and $B(\lambda)$ are found [8] to be very similar to results in the literature [18, 19] (see Fig. 5 below). The values of the long period L, which vary between 12 and 14 nm, are listed without discussion in Table I below.

2.3. Gels

The solvents chosen were either those commonly used for PE analysis (decalin and trichlorobenzene (TCB)) or chemically similar to PE such as the alkanes. The isomer of hexadecane, br-C_{16}, was added to the others since its molecular shape has been found to lead to solution properties different from those of the long linear alkanes. Relatively small differences in cohesive energy and molecular size lead to a 15 K range of T_d, the dissolution temperature for these solvents, the highest being for n-C_{16} (due to its large molecular size) and the lowest for decalin. The fact that TCB has replaced decalin as a good solvent for characterization (as in GPC analysis) seemed an interesting bit of information worthy of further investigation.

The solutions, precursors of the gels, were prepared using standard procedures [6–14]. Precautions were taken to have a solution free from degradation and homogeneous and a gel without air bubbles. Most of the gels were dried at room temperature. For the less volatile solvents, the drying was done under vacuum at a moderate temperature (40–50 °C). The i.r. spectra of the films after drying did not indicate an absorbance in the carbonyl region larger than that of the nascent sample, which was hardly visible.

3. Results and discussion

3.1. Undrawn films

Table I gives the conditions of preparation, the maximum drawability λ_{max}, the long period L, the density, the melting temperature T_m by fast differential scanning calorimetry (DSC) (600 K h^{-1}) and the corresponding enthalpy of fusion H_m. The complex traces of slow calorimetry, which cannot be described by two parameters only, are decomposed in Tables II to IV below. The values of H_m (210–231 J g^{-1}) cannot differentiate between the films, which have similar calorimetric crystallinity. Consequently, the range of drawability must reside in other aspects of the morphology. The comparable values of T_m at $v = 600\ K\ h^{-1}$ and $T_{orthorhom}$ at $v = 1\ K\ h^{-1}$ illustrate the fast kinetic of the melting of the orthorhombic crystals.

3.2. Calorimetric spectra

The part of the heat evolved at high T, $H_{high\text{-}T}$, which depends on the film is listed in the last column of Table I. The choice of $H_{high\text{-}T}$, the enthalpy evolved above the end of the melting curve of the orthorhombic crystals (137–139 °C), will be explained below. A typical trace of melting of the films at $v = 1\ K\ h^{-1}$ is given in Fig. 1. It corresponds to a film prepared in n-C_{12}. Two phase changes with a slow kinetics (126–143 and 150–168 °C) separated by a region of arrested melting (143–150 °C) can be seen besides the sharp melting endotherm of the orthorhombic crystals ($T_{orthorhom.}$ = 135 °C). Similar traces are found for the

TABLE I Characteristics of undrawn UHMWPE films cast in different solvents

Solvent	Sample No.	c g dl^{-1}	λ_{max}	L (nm)	d[a] (g cm^{-3})	Fast DSC		Slow DSC	
						T_m (°C)	H_m[b] (J g^{-1})	$T_{orthorhom.}$ (°C)	$H_{high\text{-}T}$[c] (J g^{-1})
TCB	1	1.3	60	12.0	0.9711	135.5	231	135.9	30
n-C_{12}	2	0.8	260	12.7	–	135.2	220	135.3	106
Decalin	3	2.0	145	11.9	0.9704	135.2	210	135.9	55
br-C_{16}	4	1.3	150	12.8	0.9725	135.0	215	136.2	60
Chloronaphthalene	5	1.3	230	14.0	0.9721	136.1	224	136.0	90
n-C_{16}	6	0.8	250	13.3	–	135.0	222	135.4	101

[a] Films analysed after ageing.
[b] H_m = enthalpy of melting.
[c] $H_{high\text{-}T}$ = enthalpy evolved above T = 137–139 °C (see Fig. 3).

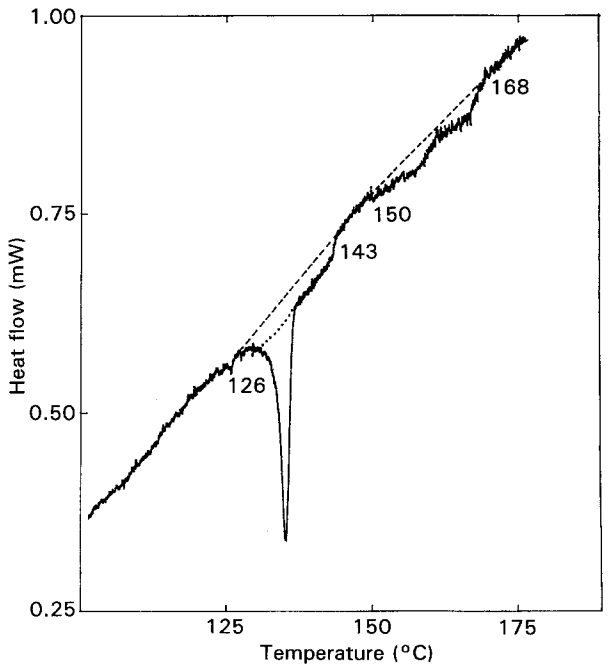

Figure 1 Melting trace at $1\,K\,h^{-1}$ of a film prepared in n-C_{12} ($m = 12.16$ mg). Note the two slow phase changes ($T = 126$–143 and 150–168 °C) and the regions of arrested melting ($T = 143$–150 °C (i.e. 7 h) and $T = 164$–165 °C).

six films, with differences in the temperature of the endotherms with slow kinetics. The position of the endotherms of fusion and the values of the enthalpies are listed in Table II where the different non-orthorhombic endotherms are associated with different degrees of strain (low, middle, high) in the chains undergoing an order–disorder transition. The distinction between low, middle and high strain-melting enthalpies is made in Table II where the different non-orthorhombic endotherms are associated with different degrees of strain (low, middle, high) in the chains undergoing an order–disorder transition. The distinction between low, middle and high strain-melting does not imply that they correspond to phases which would be distinct at room temperature. The kinetics of disordering depends on the conditions of the melting itself. The trace constitutes a calorimetric spectrum of a sample. Note that the values of the temperatures of phase changes for the non-orthorhombic morphology depend on v: they are higher for $v = 3\,K\,h^{-1}$ than for $v = 1\,K\,h^{-1}$. Descriptions of calorimetric spectra made in the same manner are found in Table IV below for some drawn films at $6\,K\,h^{-1}$.

3.3. Phase composition

Instead of describing the melting of the other films using as ordinate the heat flow as in Fig. 1, a graph of the mass fraction undergoing a phase-change versus T will be drawn from the traces as presented in Figs 2, 4 and 5 below. To transform the enthalpy change H_i; obtained over a given temperature interval T_i–T_j into fraction of polymer phase separating over this range, the enthalpy of the perfect orthorhombic crystal ($290\,J\,g^{-1}$) is used. For instance, a phase change with $29\,J\,g^{-1}$ is associated with a fraction equal to 0.1 of the sample. Since for linear PE the total enthalpy of phase change has been repeatedly found to be equal to about $290\,J\,g^{-2}$, the calorimetric analyses are consistent with an absence of any completely amorphous phase at room temperature in linear PE.

Before melting, any sample will have two phases: the orthorhombic phase whose fraction is defined by the ratio $H_{orthorhom.}/290$ and its complement, the non-orthorhombic phases identifiable by their enthalpy of phase-change. $H_{orthorhom.}$ is the first value of H listed in Tables II to IV. The orthorhombic fraction sets the first point on the phase composition diagram. The

TABLE II Analysis of the melting traces at $v = 1\,K\,h^{-1}$ of gels cast in different solvents[a]

Solvent	Sample No.	Fig.	Orthorhombic phase		Non-orthorhombic phases				
			T (°C)	H ($J\,g^{-1}$)	Low strain H ($J\,g^{-1}$)	Middle strain H ($J\,g^{-1}$)	High strain H ($J\,g^{-1}$)	Arrested melting (°C)	$T(0.8)$[b] (°C)
TCB	1	2a	135.9	195 (134–137)	20 (117–124)	45 (128–139)	30 (> 155)	124–128 139–155	132
n-C_{12}	2	1,2a	135.3	183 (132–137)	–	37 (126–143)	69 (150–168)	143–150	152
Decalin	3	2b	136.1	190 (133–139)	23 (110–119)	20 (129–138)	55 (138–150)	119–129	135
br-C_{16}	4	2b	136.2	180 (132–139)	–	50 (121–139)	40 (140–157)	139–140	138
Chloro-naphthalene	5	2b	136.2	180 (128–139)	20 (122–132)	54 (139–153)	36 (153–170)		145
n-C_{16}	6	2b	135.4	180 (132–137)	–	6 (130–137)	101 (143–156)	137–143 –	152

[a] Gels were analysed after ageing. Data were obtained from traces such as Fig. 1 and used for making the phase-content analysis of Fig. 2. The numbers in parenthesis limit the temperature interval used for integration. The total enthalpy of phase change is $280 \pm 10\,J\,g^{-1}$ for all the samples.

[b] The temperature at which a fraction of the sample equal to 0.2 is not yet melted.

phase composition of the film in n-C_{12} is plotted in Fig. 2a (curve 2). On raising T, a horizontal line corresponds to a constant phase composition and a slanted line to a phase change. The bottom part of the figure relates to the orthorhombic part and the upper part to the non-orthorhombic fraction of the sample. The fraction of the ordered non-orthorhombic phases at a given temperature is equal to the complement to unity of the ordinate of the line in the upper part of the diagram at that temperature. The orthorhombic fraction diminishes to 0 between 132 and 137 °C and is replaced by an isotropic melt. The non-orthorhombic phases disorder slowly and by steps between 126 and 168 °C. The film starts to undergo a phase change at 126 °C which continues up to 143 °C. Melting is arrested (horizontal line) between 143 and 150 °C. Melting resumes up to 168 °C but is interrupted for 1–2 K at 164–165 °C. If a similar diagram were made from the fast DSC results, it would show only the trace in the lower part corresponding to the melting of the orthorhombic crystals over a narrow T range, and this part would not be different from the trace obtained from slow DSC analysis. A horizontal line of crosses is drawn above 160 °C in Figs 2 and 4 as a reminder of the heterogeneity of the melt. The latter is revealed by the two-exotherm crystallization trace obtained on cooling. The kinetics of crystallization in a slow-T ramp bears a resemblance to that of fusion, being slow for the high-T exotherm and rapid for the growth of orthorhombic crystals [2].

In Fig. 2a the calorimetric spectrum of the film in TCB has been added (curve 1) to that of the film prepared in n-C_{12} (curve 2) to illustrate the difference in phase changes at high T between two films whose value of λ_{max} is different. Fig. 2b corresponds to the same analysis for the films in decalin (curve 3), br-C_{16} (curve 4), chloronaphthalene (curve 5) and n-C_{16} (curve 6).

One sees that the lower part of the phase composition does not differ much between the samples. The large difference resides in the temperatures at which the high-T phase changes occur. The temperature at which the unmelted part of the non-orthorhombic material corresponds to 0.8 of the total heat; the point with 0.8 as ordinate called $T(0.8)$ can be used as an indicator of the sample melting characteristics. $T(0.8)$ is about 135 °C for curves 3 and 4, 145 °C for curve 5 and 150 °C for curve 6. As seen in Fig. 1, some ambiguity exists in separating the low-T phase change from the fusion of the orthorhombic crystals, but usually none in defining the high-T phase change.

3.4. Temperature of phase changes and drawability

The conditions to obtain a high drawability have been studied extensively. The parameters investigated [6, 7, 9–21] were related to the solution (solvent, concentration, shear during stirring), to the conditions of crystallization and drying of the films and to the temperature of drawing. Information such as the high drawability of single-crystals mats [22] of high MW or the difference in drawability of nascent polymer and recrystallized polymer [23] convey the idea that high (or medium) drawability can be achieved through a balance of opposite effects. At the drawing temperature, the sample must be neither too soft nor too hard and the concentration of entanglements must be optimum as reported in the literature. Comparison of the λ_{max} values with the upper part of Fig. 2b for the different solvents suggests that the higher the temperature of phase separation, the more drawable is the film. Since the total heat of phase change is the same for all the films, the range of temperature of phase change can be replaced, as an indicator of toughness of the film, by the heat not yet evolved at a given temperature. The temperature of 120 °C is not suitable to differentiate the samples because at that temperature too little of the non-orthorhombic phase change has been evolved. Instead the end temperature of the melting peak of the orthorhombic material, i.e. $T = 137$–139 °C, is used. The value of λ_{max} has been plotted against $H_{high\text{-}T}$ (the heat effect above 137–139 °C) in Fig. 3.

The good correlation between the two variables indicates that, in the present drawing and calorimetric experiments, $H_{high\text{-}T}$ gives useful information for understanding the conditions required for high drawability. The softening of the film starts below the temperature of phase change, probably as low as the

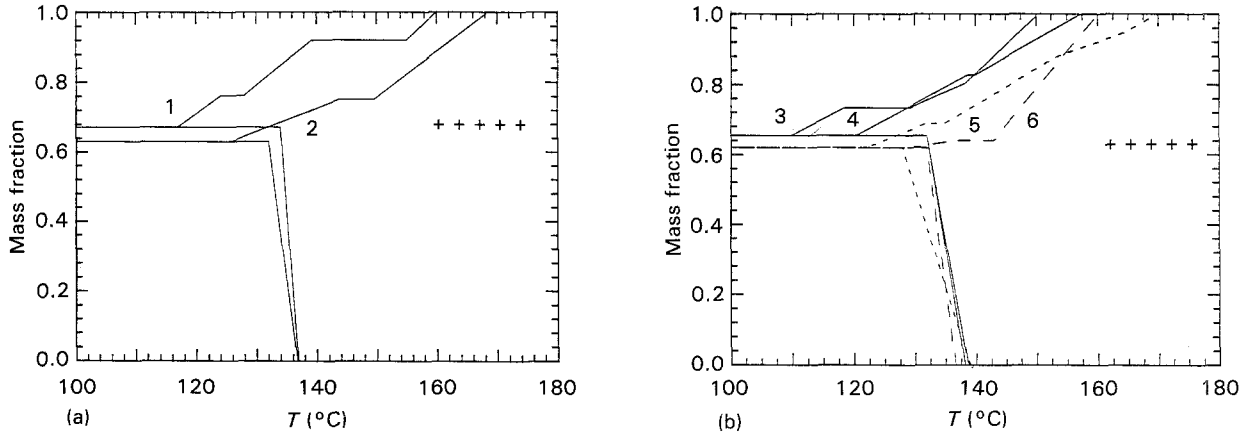

Figure 2 Phase content versus T of the films: (a) in TCB (curve 1) and n-C_{12} (curve 2), two solvents with the extreme values of λ_{max}; (b) in decalin (curve 3), br-C_{16} (curve 4), chloronaphthalene (curve 5) and n-C_{16} (curve 6). The upper part of the graphs is the distinctive part (see text). The crosses at high T are a reminder of the persistent heterogeneity of the melt.

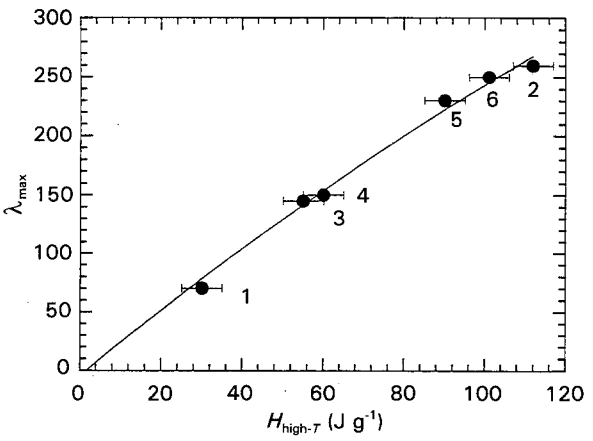

Figure 3 Correlation between λ_{max} and $H_{high\text{-}T}$ in six solvents. $H_{high\text{-}T}$ is the heat effect at $T > 137$–139 °C. Numbers as in Table I.

drawing temperature. The film in TCB is not highly drawable at 120 °C, probably because it is too soft as indicated by the 20 J g^{-1} endotherm evolved between 117 and 124 °C in a 1 K h^{-1} temperature ramp. It is possible that if drawing were to be achieved at a lower T (20 K lower), the TCB film would draw as well as the film in n-C_{12} due to the right conditions of hardness and entanglement concentration. More will be said on the subject at the end of this paper where the presence of a physical network in the same is discussed. The manner in which $H_{high\text{-}T}$ has been evaluated can be followed in Table II. When $T = 137$–139 °C is at the beginning of an endotherm or in a region of arrested melting, the evaluation of $H_{high\text{-}T}$ is straightforward for curves 1, 3 and 6: $H_{high\text{-}T}$ is about equal to the value given in the last column (with high-strain heading). For curves 2 and 5, $H_{high\text{-}T}$ is the sum of the last two columns and for curve 4, part of the middle-strain endotherm only has been added. A similar correlation is obtained if $T(0.8)$ is used in Fig. 3 instead of $H_{high\text{-}T}$.

3.5. Phase composition and conditions of crystallization

If the replacement of a solvent by another can lead to the range of phase content observed in the films analysed in Fig. 2a and b, one can expect that other thermal histories will have important effects. Crystallization from the melt of the same UHMWPE has been done and the melting trace obtained at 1 K h^{-1}. The location and size of the endotherms on the melting trace are given in Table III. The first row corresponds to the melting of nascent UHMWPE, the second to that of the recrystallized sample, the third and fourth to the melting of a Marlex sample ($M_W = 150\,000$) and of a sample of narrow MW distribution ($M_W = 119\,000$). The phase contents are given in Fig. 4. In Fig. 4a the crystallinity of the UHMWPE is seen to increase due to the treatment, as expected. The most striking result is the change in the non-orthorhombic phase changes brought about by the fusion–crystallization. While the nascent sample (curve 1) melts almost continuously between 120 and 175 °C, the recrystallized sample shows arrested melting over a long T interval (121–125, 138–154 °C). The values of $T(0.8)$ are respectively 151 and 162 °C. The strain in the sample, which raises the temperature of phase change, has increased considerably. Furthermore, recrystallization has created in the sample regions of high and low strain which were not present in the nascent PE.

The trace of the recrystallized sample illustrates the fact that the entire calorimetric spectrum must be analysed to draw conclusions on drawability. However, the correlation of Fig. 3, which is suitable for comparing samples with very similar treatment such as the present films, has its limits because it does not include for instance the range of arrested melting. If used for the recrystallized film which has an $H_{high\text{-}T}$ value of 95 J g^{-1}, it would predict an unrealistically high drawability.

The effect of melting–recrystallization is less dramatic when the sample has a lower MW and when the thermal history is shorter than that used for UHMWPE. For Marlex $T(0.8)$ is 156 °C, i.e. an intermediate value between those for nascent and recrystallized UHMWPE; $T(0.8)$ is 130 °C for the monodisperse sample. The present results are in agreement

TABLE III Analysis of the melting traces at $v = 1$ K h^{-1} of samples of different MW and treatment

Solvent	Sample No.	Fig.	Orthorhombic phase		Non-orthorhombic phases				
			T (°C)	H (J g^{-1})	Low strain H (J g^{-1})	Middle strain H (J g^{-1})	High strain H (J g^{-1})	Arrested melting (°C)	$T(0.8)$[b] (°C)
Nascent Gur[a,d]	1	4a	139.3	150 (134–142)	49 (119–137)	58 (142–157)	20 (162–168) (> 168)	157–162 –	151
Melt (recrystallized)[b]	2	4a	134.3	168 (125–138)	26 (108–121)	65 (154–167)	30 (167–174)	121–125 138–154	162
Marlex[c]	3	4b	132.5	200 (122–133)	11 (122–140)	–	81 (152–167)	133–152	156
NIST 1484[d]	4	4b	132.0	232 (128–136)	30 (124–130)	32 (138–146)	–	136–138	130

[a] Decomposition used for Fig. 4a.
[b] Very long thermal history (0.5 K h^{-1} for melting, 1 K h^{-1} for crystallization).
[c] As received (pellets).
[d] As received (powder).

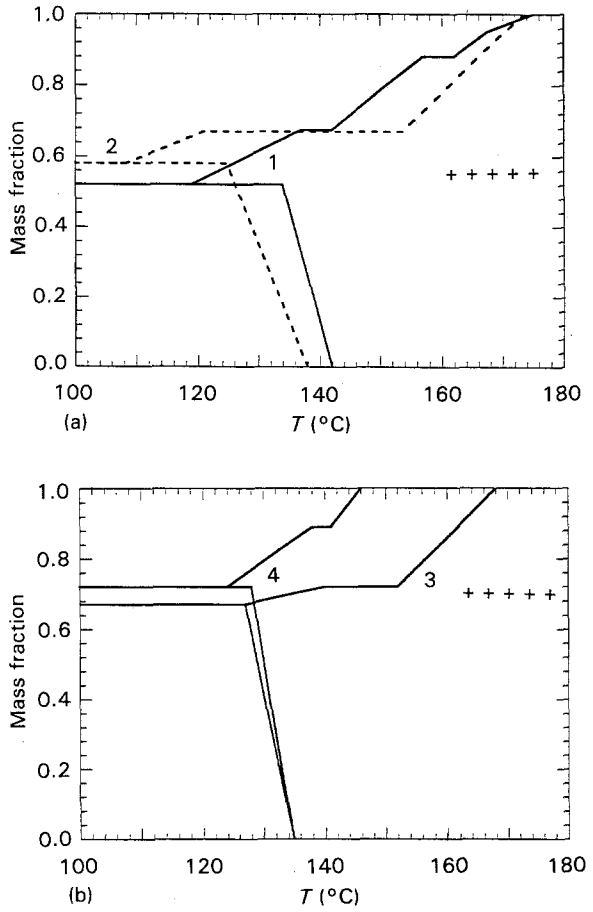

Figure 4 Phase content versus T, effect of sample thermal history of MW. (a) Curves 1 and 2 are for PE Gur nascent and after slow melting and crystallization. Note the change in the non-orthorhombic phase brought by the treatment. (b) Curve 3 is for $M_W = 150\,000$ (Marlex) and curve 4 for $M_W = 119\,000$ (NIST 1484), both melted as received.

with other investigations giving a primary role to the non-crystalline phase in the deformation of HMWPE. The fact that nascent UHMWPE is more drawable ($\lambda_{max} = 50$) [23] than the recrystallized sample ($\lambda_{max} = 5$) reflects the difference in their calorimetric spectra and the correlation proposed above between drawability and high-T phase changes.

3.6. Origin of the high-T endotherms

In the text above, the high-T endotherms have been associated with non-orthorhombic crystals because, at T_m, the X-ray scattering which is characteristic of the orthorhombic crystals disappears. The order which is destroyed by slow heating cannot come from small and strain-free crystals. If this were the case, they would melt below T_m. It is reasonable to assume that the high-T endotherms correspond to the melting of crystals deformed by strain and whose order is too short-range to be seen by X-ray scattering. The origin of that strain and its stability after the fusion–dissolution of the orthorhombic crystals have been the subject of further thought. In a recent paper, [24] we propose that the non-orthorhombic phase changes with a slow kinetics observed at high and low temperature are order–disorder transitions in physical networks. The physical network is created at the first melting of a nascent sample, the large expansion on melting transforming a fraction of the loose knots formed during the polymerization and first crystallization of the nascent sample into very tight knots which bond the chains into a network.

Arguments for an irreversible change during the melting of the nascent polymer are based on three experimental results from (i) ^{13}C NMR spectra, (ii) dissolution in some solvents and (iii) slow melting of networks obtained through a chemical reaction:

(i) The observation that the ^{13}C NMR spectrum of nascent PE has a single peak and that of the recrystallized PE has two suggests that melting–crystallization changes the phase content;

(ii) in some solvents, tightening of the knot appears to be delayed because the full heat of fusion is evolved in the main peak, and

(iii) a large high-T endotherm is found for chemically cross-linked samples.

The traces of Fig. 4a, which show a phase composition so different for the nascent and for the recrystallized samples, support also the role of the first melting and subsequent crystallization in modifying the morphology of the sample. Current work on the variation of the ^{13}C NMR spectra with temperature confirms the different melting processes in the nascent and recrystallized samples. The unique spectra characteristic of the nascent polymer have been found for linear PEs of different molecular weights.

The presence of a network is consistent with the present results. The melting trace allows us to define the parameters characteristic of the network, namely the non-orthorhombic enthalpy of phase change and the range of temperature in which it disorders. Drawing is possible without chain-breaking if the network is distributed regularly in the sample and if it is still sufficiently ordered at the drawing temperature used. The higher strain is released during deformation because of chain slippage and also probably through breaking of bonds in the already strained parts of the material. The role of the solvent is being investigated systematically. It appears that the conditions of the first dissolution of the nascent sample which define the network characteristics, i.e. nature of the solvent [8b] and concentration, are important factors in the phase composition of the film after crystallization and drying. The melting and dissolution traces are used to quantify the effect of different parameters on the overall strain and its re-partitioning in the sample.

3.7. Other techniques for measuring the phase composition

The parts of the sample which undergo phase changes at high T (i.e. the ordered parts of the network) are revealed by their ability to be disordered on heating. The special morphology should be seen at room temperature by other techniques sensitive to chain mobility; ^{13}C NMR of PE has been done at room temperature on samples with different thermal history [25]. Analysis of the spectrum leads to its decomposition into three components: the crystalline component

(33.0 p.p.m), the interfacial component (31.3 p.p.m.) and the rubber component (31.0 p.p.m.). In a high-MW sample crystallized from the melt, the proportions of the three phases are respectively 66, 18 and 16%. In the decomposition, the p.p.m. values of the two non-orthorhombic phases cover a large range indicative of the heterogeneity of these phases. The calorimetric trace, which obviously does not detect completely random chains, can nevertheless identify three phases to match those found by ^{13}C NMR. The distinction between the two non-orthorhombic phases rests on their temperature of phase change. For example, in curve 2 of Fig. 2a, the fraction which undergoes a phase change at low T (i.e. between 126 and 143 °C) can be associated with the phase which has the highest NMR mobility, labelled the rubbery phase. On the other hand, the fraction which melts between 150 and 168 °C should correspond to the interlamellar phase of intermediate mobility. The respective fraction of these two mobile phase depends on the solvent used for the film preparation but ranges around the values quoted by Kitamaru *et al.* [25]. A similar analysis has been made with solution-crystallized Marlex and the result compared to the ^{13}C NMR data on a solution-crystallized sample ($M_W = 91\,000$) [25]. The changes to the phase composition brought about by the crystallization in solution are found to be the same by calorimetry and by NMR. The more mobile phase has decreased to the benefit of the interlamellar phase while the crystalline phase has hardly changed. A more definite analysis requires the comparison by the two techniques of the same samples having been submitted to the same thermal history. An analysis of the phase composition of the melt of medium-MW PE using proton NMR spin–spin relaxation measurements published recently [26] arrives at conclusions very similar to those deduced from slow calorimetry concerning the presence of order in the melt. The phase changes in the melt can be the physical reason behind the findings of a temperature window [27] of drawability for PE melts. A comparison of the temperature ranges for high drawability and arrested melting, for instance, is not feasible now because the effects observed in drawing and slow fusion are dependent on the conditions of measurement.

3.8. Drawn films

Drawn films have been studied by a variety of techniques [28, 29] to understand their mechanism of deformation [17], their morphology, their crystallinity [18, 22] and most importantly their unique mechanical properties [9–19]. Although drawing aligns the chains as seen by the decrease of the concentration of gauche bonds [22], the overall morphology of a drawn film remains complex and different [28] from the extended-chain morphology obtained by crystallization under pressure. Data obtained from fast DSC, density, X-ray diffraction and NMR show an increase of crystallinity with λ, an increase which is rapid for $\lambda < 50$ and slow for higher λ. Drawing also raises the value of T_m and generates a multi-peak melting trace. The density of drawn films increases towards the density of the orthorhombic crystals but diminishes for higher draw ratios. Our inquiry was aimed at finding the response to drawing of the calorimetric spectra, particularly of the high-T part which had not been investigated before.

In the present work the birefringence B, Young's modulus E, density, fast and slow calorimetry traces have been measured on drawn films. The curves of B and E versus λ indicate that there is little solvent effect on B and E, the magnitude of which is principally determined by λ. The curves $B(\lambda)$ and $E(\lambda)$, which are very similar to published curves [16–20], will not be discussed here but the results are given in Fig. 5.

The melting traces of the drawn fibres by fast DSC give results similar to those found in the literature. The enthalpy of melting increases (from about 210 to 260 J g^{-1}) and the melting trace has several peaks. In slow melting, the total enthalpy is unchanged by drawing but the temperatures of phase changes are modified: the temperatures of the phase changes of the non-orthorhombic parts diminish while $T_{orthorhom.}$ is raised. After drawing, the kinetics of phase change are respectively slower for the orthorhombic and faster for the non-orthorhombic phases than before drawing. The calorimetric trace indicates that the phases present in the drawn films are less different from each other in their melting properties than they were in the undrawn ones. Curves 1, 2 and 3 of Fig. 6 are the

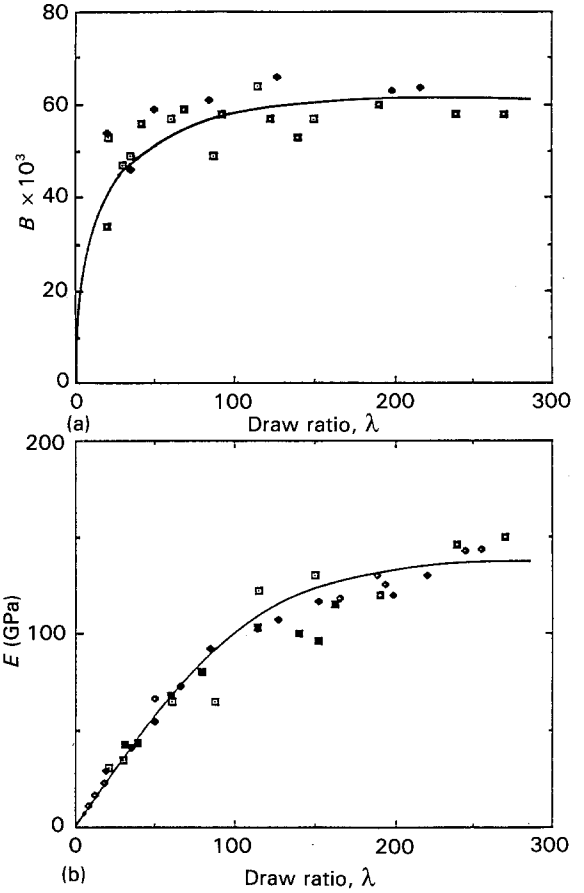

Figure 5 Variation of (a) birefringence B and (b) Young's modulus at 25 °C versus draw ratio λ for films prepared from solutions (■) 2% in decalin, (◆) 1.3% in n-C12, (⊡) 0.8% in n-C12, (◇) 0.8% in n-C16, (⊡) 1.3% in b-C16.

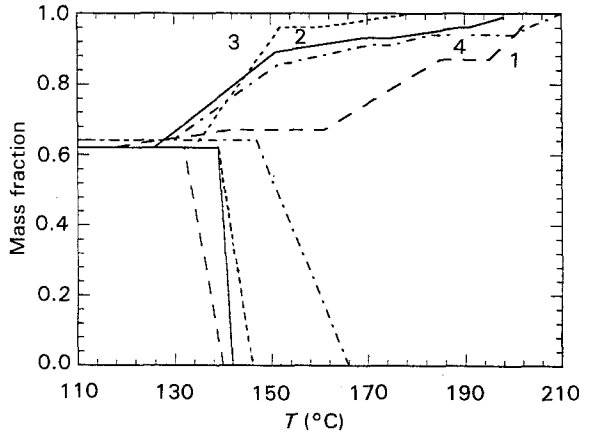

Figure 6 Phase content versus T of drawn films from melting traces at 6 K h^{-1}. Curve 1 is for $\lambda = 1$, curve 2 for $\lambda = 19$, curve 3 for $\lambda = 200$, curve 4 is from the melting trace at 600 K h^{-1} for $\lambda = 200$. See text for explanation.

calorimetric phase composition of 6 K h^{-1} of the films undrawn (curve 1) and drawn with $\lambda = 19$ and $\lambda = 200$ (curves 2 and 3). The detailed decomposition of the melting trace is given in Table IV. The displacements mentioned above are particularly remarkable between the undrawn film (curve 1) and the film with $\lambda = 19$ (curve 2). Note that the temperature of the phase changes in the non-orthorhombic part of the undrawn film are higher than in the previous figures because of the rate of heating, which is six times higher. To illustrate the weakening effect of drawing on the non-orthorhombic phase, a highly drawn film ($\lambda = 200$) was melted in fast DSC and its phase composition compared to that obtained with the slow DSC trace. The high-T phase change occurs so fast for the drawn film that the corresponding line (curve 4) overlaps that for $\lambda = 19$ obtained from the trace of slow DSC. A small fraction of the film does not melt by fast DSC. These results mean that a loss of entanglements and of strain occurs during drawing due to chain slippage and chain breaking. Other investigators arrived at the same conclusion without comparing slow and fast calorimetry [30].

3.9. Constrained melting

Drawn films were melted under constraint by fast and slow DSC. Fast DSC shows an increase of the temperature of the endotherm of fusion. In slow DSC, the high-T endotherms are very similar to those of the undrawn, unconstrained films with regions of arrested melting. The built-in strain of the sample, released by drawing, has been reformed by the imposition of a mechanical strain. The crystallization trace shows also two phase changes with different kinetics, but the high-T exotherm is larger than its counterpart in the melting trace. The trace reflects the different mode of crystallization of a sample submitted to conditions in which chain-scission and cross-linkings have been observed [30]. It is likely that part of the larger high-T exotherm corresponds to the ordering of chains now bonded by covalent bonds.

4. Conclusion

Slow melting of films reveals high- and low-T phase changes not observed by fast DSC. Knowing their enthalpy and temperature, a phase composition of the sample can be drawn. That phase composition consists of the orthorhombic part and a non-orthorhombic part. The phase compositions of films prepared in different solvents indicate that the non-orthorhombic fraction is solvent-dependent. The value of maximum drawability λ_{max} is found to vary over a large range with the solvent used for preparing the film. One can relate good drawability to a special range of T of phase change for a given drawing temperature. Melting and recrystallization profoundly change the phase composition of the nascent sample, since the process introduces phase heterogeneity in the material with regions of arrested melting. Drawing a sample weakens the strain of the sample so that the high-T phase changes observed on undrawn films by slow DSC can be seen by fast DSC, seemingly increasing its crystallinity. The origin of the strain in the sample could be a network formed in the nascent sample at the first fusion/dissolution.

TABLE IV Analysis of the melting traces at $v = 6$ K h^{-1} of drawn films (Fig. 6)

Solvent	Sample No.	v (Kh^{-1})	λ	Orthorhombic phase		Non-orthorhombic phases			
				T (°C)	H (J g^{-1})	Low strain H (J g^{-1})	Middle strain H (J g^{-1})	High strain H (J g^{-1})	Arrested melting T (°C)
n-C_{12}	1	6	1	134.8	180 (132–140)	15 (118–142)	58 (154–183)	17 (200–210)	142–154 183–200
Decalin	2	6	19	141.0	180 (139–142)	78 (126–151)	12 (151–169)	14 (175–189) 10 (191–198)	169–175 – 189–191
n-C_{12}	3	6	200	143.4	180 (142–146)	98 (134–152)	11 (160–180)	–	152–160
n-C_{12}^{a}	4	600	200	154.3	186 (147–166)	64 (129–152)	14 (157–170)	9 (175–183)	–

[a] Decomposition is unsure when there is no arrested melting.

Slow calorimetry seems to be a useful technique to contribute to the understanding of the melting, crystallization and deformation of crystals.

Acknowledgements

We acknowledge the support of the National Research Council of Canada. We thank Dr J. Prudhomme (Université de Montréal) for advice in measurements on films and Dr I. Lapes for discussion and calorimetric experiments.

References

1. H. PHUONG-NGUYEN and G. DELMAS, *Macromolecules* **30** (1992) 414.
2. *Idem, ibid.* **30** (1992) 408.
3. *Idem, Thermochim. Acta* (1994).
4. P. BERNAZZINI, M.Sc. Thesis, (UQAM, Montreal, 1994).
5. X. ZHANG, I. LAPES, H. PHUONG-NGUYEN, unpublished work.
6. A. ZWIJNENBURG and A. J. PENNINGS, *Colloid Polym. Sci.* **253** (1975) 452.
7. *Idem, ibid.* **254** (1976) 868.
8. H. PHUONG-NGUYEN, PhD thesis, McGill University, Canada (1991).

8b. H. PHUONG-NGUYEN and G. DELMAS, *J. of Solution Chem.* **23** (1994) 249.

9. P. J. BARHAM and A. KELLER, *Polym. Lett.* **17** (1979) 591.
10. *Idem, ibid. J. Mater. Sci.* **15** (1980) 2229.
11. P. SMITH and P. J. LEMSTRA, *Makromol. Chem.* **180** (1979) 2983.
12. *Idem, J. Mater. Sci.* **15** (1980) 505.
13. *Idem, Polymer* **21** (1980) 134.
14. *Idem, J. Colloid Polym. Sci.* **258** (1980) 891.
15. W. T. MEAD, C.R. DESPER and R. S. PORTER, *J. Polym. Sci., Polym Phys. Ed.* **17** (1979) 859.
16. G. CAPACCIO, A. G. GIBSON and I. M. WARD, in "Ultra High Modulus Polymers", edited by A. Cifferi and I. M. Ward (Applied Science, London, 1979) p. 1.
17. H. Van Der WERFF and A. J. PENNINGS, *Colloid Polym. Sci.* **269** (1991) 747.
18. T. OGITA, N. SUZUKI, Y. KAWAHARE and M. MATSUO, *Polym. J.* **33** (1992) 698.
19. C. SAWATARI, T. OKUMURA and M. MATSUO, *Polym. J.* **18** (1986) 741.
20. T. OGITA, N. SUZUKI, F. OZAKI and M. MATSUO, *Polymer* **32** (1991) 822.
21. T. KANAMOTO, K. TSURUTA, K. TANAKA, M. TAKEDA and R. S. PORTER, *Polym. J.* **15** (1983) 327.
22. K. FURUHATA, T. YOKOKAWA, Ch. SEOUL and K. MIYASAKA, *J. Polym. Sci., Polym. Phys. Ed.* **24** (1986) 59.
23. L. H. WANG, S. OTTARI and R. S. PORTER, *Polymer* **32** (1991) 1776.
24. G. J. DELMAS, *Polym. Sci., Polym. Phys. Ed.* **31** (1993) 2011.
25. R. KITAMARU, F. HORII and K. MURAYAMA, *Macromolecules* **19** (1986) 636.
26. T. BREMMER and A. RUDIN, *J. Polym. Sci. Polym. Phys. Ed.* **30** (1992) 1247.
27. A. J. WADDON and A. KELLER, *ibid.* **28** (1990) 1063.
28. J. CLEMENTS, G. CAPPACIO and I. M. WARD, *J. Polym. Sci., Polym. Phys. Ed.* **17** (1979) 693.
29. N. S. MURPHY, S. T. CORREALE and S. KAVESH, *Polym. Commun.* **31** (1990) 50.
30. J. SMOOK and A. J. PENNINGS, *Colloid Polym. Sci.* **262** (1984) 712.

Received 15 December 1993
and accepted 19 January 1994